Thermochemical Studies of $LnBa_2Cu_3O_{7-\delta}$ (*Ln* = Pr, Nd, Eu, Gd, Dy, Ho, Tm), $LnBa_2Cu_4O_8$ (*Ln* = Sm, Eu, Gd, Dy, Ho), and $Y_{1-x}Pr_xBa_2Cu_3O_{7-\delta}$

V. E. Lamberti,* M. A. Rodriguez, J. D. Trybulski, and A. Navrotsky

Princeton Materials Institute and the Department of Geosciences, Princeton University, Princeton, New Jersey 08544

H. B. Liu

Department of Materials Science and Engineering, Massachusetts Institute of Technology, Cambridge, Massachusetts 02139

Received September 23, 1996. Revised Manuscript Received January 27, 1997[⊗]

Employing oxide-melt drop-solution calorimetry, we have performed the first comparative thermochemical investigations of the title compounds. The enthalpies of formation of the Ln123 derivatives display an essentially linear trend toward less exothermic values with increasing lanthanide atomic number, implying that these phases become more stable with increasing lanthanide radius. In contrast, the enthalpies of oxidation vary to only a minor extent with the choice of lanthanide and suggest that the chain-site charge distributions of the Ln123 are comparable. The thermodynamic characteristics of Pr123 generally follow the trends established by the other Ln123 and reveal no gross energetic anomaly associated with the suppression of superconductivity. The enthalpies of formation of the Ln124 derivatives manifest a maximum at Gd124, while the unit-cell volumes and enthalpies of drop-solution and formation of these compounds are nearly constant multiples (2.3, 1.6−1.7, and 1.3−1.4, respectively) of the corresponding parameters of the Ln123 derivatives. The enthalpies accompanying the reactions Ln123(s) + CuO(s) → Ln124(s) imply that the Ln124, like Y124, are stable with respect to an assemblage of the fully oxygenated 123 phase and CuO. The data for the (Y,Pr)123 solid solutions are continuous across the join, arguing against any sudden *x*-dependent valence instability, but display asymmetric deviations from ideal solution behavior that can be modeled satisfactorily within the subregular approximation. Perhaps most intriguingly, the superconducting critical temperatures and the enthalpies of oxidation of the (Y,Pr)123 solid solutions are linearly related.

Introduction

As the number and commercial potential of high-temperature superconductors (HTS) have grown, so have the efforts to gain a unified understanding of their physical and critical properties, their phase equilibria, and their compatibility with other materials and the environment. In pursuit of readily manufactured new materials with less anisotropy and ever greater critical temperatures, investigators have increasingly focused on the connections between the bulk properties and the microstructures of the HTS. Underlying this perspective, however, is the recognition that microstructure depends upon processing and that processing, in turn, rests upon thermodynamic and kinetic foundations.[1]

Thermodynamic constraints on a material are generally derived through calorimetric or electromotive force (emf) measurements, phase equilibria studies, or determinations of thermal expansivity or volume compressibility. We have, for example, utilized oxide-melt calorimetry to demonstrate that $YBa_2Cu_3O_{7-\delta}$ (Y123) is unstable with respect to corrosion by water vapor and carbon dioxide at room temperature,[2] and Lindemer[3] et al. have constructed the 123−CuO section of the Y_2O_3−BaO−CuO phase diagram by thermogravimetric determinations of the temperature and oxygen pressure conditions necessary for decomposition of $YBa_2Cu_3O_{7-\delta}$ and $YBa_2Cu_4O_8$ (Y124).

In this paper, we return to oxide-melt calorimetry and present the first comparative thermochemical investigations of $LnBa_2Cu_3O_{7-\delta}$ (*Ln* = Pr, Nd, Eu, Gd, Dy, Ho, Tm), $LnBa_2Cu_4O_8$ (*Ln* = Sm, Eu, Gd, Dy, Ho), and $Y_{1-x}Pr_xBa_2Cu_3O_{7-\delta}$ (x = 0.0, 0.1, 0.2, 0.5, 0.8, 0.9, 1.0). We have measured the enthalpies of drop-solution into $Pb_2B_2O_5$ of these compounds and, employing thermochemical cycles and data from the literature, calculated their enthalpies of formation, the partial molar enthalpies of oxidation for the 123-class materials, and the enthalpy changes accompanying the reactions Ln123(s) + CuO(s) → Ln124(s), all at 298 K. We discuss these thermodynamic quantities, along with a number of structural parameters, in terms of the relative stabilities and unit-cell charge distributions of the HTS and in terms of the 123−124 phase equilibria.

Much of this study was inspired by the unusual physical and structural properties of Pr123[4] —including,

[⊗] Abstract published in *Advance ACS Abstracts,* March 15, 1997.

(1) Beyers, R.; Ahn, B. T. *Annu. Rev. Mater. Sci.* **1991**, *21*, 335.
(2) Zhou, Z.; Navrotsky, A. *J. Mater. Res.* **1993**, *8*, 3023.
(3) Lindemer, T. B.; Washburn, F. A.; MacDougall, C. S.; Feenstra, R.; Cavin, O. B. *Physica C* **1991**, *178*, 93.
(4) Radousky, H. B. *J. Mater. Res.* **1992**, *7*, 1917.

S0897-4756(96)00492-9 CCC: $14.00

Table 1. Oxygen Contents and Structural Characteristics of $LnBa_2Cu_3O_{7-\delta}$ Compositions

Ln	$7-\delta$[a]	a (Å)	b (Å)	c (Å)	V (Å^3)	$100D$[b] (Å)
Pr	6.955(5)	3.8587(2)	3.9302(1)	11.7126(3)	177.62(1)	7.15(2)
Nd	6.933(12)	3.8598(3)	3.9158(4)	11.7544(7)	177.66(2)	5.60(5)
Eu	6.962(6)	3.8437(5)	3.9040(7)	11.7191(13)	175.85(3)	6.04(9)
Gd	6.972(7)	3.8375(5)	3.9011(7)	11.7107(14)	175.31(3)	6.36(9)
Dy	6.939(6)	3.8269(5)	3.8923(7)	11.6904(13)	174.13(3)	6.54(9)
Ho	6.941(4)	3.8204(5)	3.8881(7)	11.6810(11)	173.51(3)	6.77(9)
Tm	6.951(7)	3.8108(7)	3.8827(6)	11.6721(16)	172.70(3)	7.18(9)

[a] Error obtained through propagation of twice the standard deviation of the mean. [b] Orthorhombic distortion, $b - a$.

most notably, the singular absence of superconductivity among all the rare-earth analogues of Y123.[5,6] [For convenience in exposition, however, we sometimes include the Pr-containing compounds among the HTS and the (Y,Pr)123 solid solutions among the Ln123.] Hence, we also emphasize thermodynamic, structural, and critical correlations between Pr123 and the other rare-earth derivatives of Y123 and discuss the mixing properties of the (Y,Pr)123 series in some detail. In addition, we provide evidence of a linear relationship between the superconducting critical temperatures and the partial molar enthalpies of oxidation of the (Y,Pr)-123 solid solutions. Portions of the data centering on praseodymium and high-temperature superconductivity have been published previously.[7]

Experiments

Synthesis of 123 Series. Polycrystalline $Ln Ba_2Cu_3O_{7-\delta}$ (Ln = Pr, Nd, Eu, Gd, Dy, Ho, Tm) and $Y_{1-x}Pr_xBa_2Cu_3O_{7-\delta}$ (x = 0.0, 0.1, 0.2, ..., 1.0) were prepared from AEsar/Johnson Matthey Ln_2O_3 (M3N5−M5N), Y_2O_3 (M5N), Pr_6O_{11} (M4N), $BaCO_3$ (M4N), and CuO (M5N). (The Pr123 end-member was a sample of the material used in our earlier diffraction study.[8]) The starting materials were dried at either 473 (carbonate) or 1073 K (oxides). For each composition, the reactants were grouped stoichiometrically in an agate mortar, ground to a visibly homogeneous mixture, and then pelleted into half-gram disks of diameter 1.3 cm. The pellets were prefired in air for 15 h at 1123 K and then calcined for at least 168 h at 1183−1213 K. Polycrystalline magnesia or platinum crucibles were utilized in all thermal processing steps. Cycles of grinding and pelletization were performed after the prefiring and at regular intervals during the calcination until X-ray diffraction patterns (vide infra) displayed no signs of starting materials or common impurities such as $BaCuO_2$ or the 211 phases.

The black calcination products were annealed for 48−64 h at 673 K in flowing oxygen and then slowly cooled (10−20 K min^{-1}) to room temperature. This treatment resulted in values of δ less than 0.07. Samples with lower oxygen contents, needed for the determination of the heats of oxidation, were prepared through reequilibration at higher temperatures in flowing oxygen and subsequent quenching into liquid nitrogen. The values of δ for the low-oxygen-content materials ($0.4 < \delta < 0.5$) were chosen to avoid the Y123-like orthorhombic → tetragonal phase transition that was observed in all lanthanide derivatives and (Y,Pr)123 solid solutions upon deoxygenation. (In practice, the oxygen content corresponding to the transition point depended in a more or less unpredictable manner upon the occupant(s) of the yttrium site, requiring that the orthorhombicity of each low-oxygen-content sample be confirmed by means of X-ray diffraction.) The oxygen contents ($7-\delta$) of the final products were determined by iodometric titration against KIO_3-standardized $Na_2S_2O_3$ (vide infra). All products—including the 124-class derivatives discussed in the next section—were stored over $CaSO_4$ desiccant until needed in order to avoid degradation through reaction with atmospheric water or carbon dioxide.[2]

Table 2. Structural Characteristics of $LnBa_2Cu_4O_8$ Compositions

Ln	a (Å)	b (Å)	c (Å)	V (Å^3)	$100D$[a] (Å)
Sm	3.8703(3)	3.8873(3)	27.3107(18)	410.89(4)	1.70(4)
Eu	3.8676(5)	3.8842(4)	27.2928(26)	410.01(6)	1.67(6)
Gd	3.8625(4)	3.8825(4)	27.2756(24)	409.04(5)	2.00(6)
Dy	3.8478(3)	3.8752(3)	27.2454(20)	406.26(4)	2.74(4)
Ho	3.8444(3)	3.8725(3)	27.2410(16)	405.55(3)	2.81(4)

[a] Orthorhombic distortion, $b - a$.

Synthesis of 124 Series. Polycrystalline $Ln Ba_2Cu_4O_8$ derivatives (Ln = Sm, Eu, Gd, Dy, Ho) were prepared from M5N-purity AEsar/Johnson Matthey Ln_2O_3, BaO_2, and CuO. All starting materials were dried at 473 K for 24 h. For each composition, the reactants were grouped stoichiometrically in an agate mortar, ground to a visibly homogeneous mixture, and then pressed into cylinders measuring 0.6 cm in diameter. The cylinders were fired for 15 h at 1223 K under 220 bar O_2, after which they were pulverized and recompacted and then fired for an additional 60 h under the same conditions. Polycrystalline gold substrates were utilized in all thermal processing steps. X-ray diffraction patterns revealed minor CuO components in all members of the series, as well as a number of other minor impurities, including most probably the Ln211 phases and $Ba_2Cu_3O_{5.9}$, in the Dy and Ho congeners. Following Zhou and Navrotsky,[9] we believe that these impurities do not significantly degrade our results.

Iodometric Titration.[9−12] A powdered 123-series sample, with mass typically in the range 25−30 mg, was placed under a flowing inert atmosphere (Ar or N_2) in a three-mouthed flask. The sample was covered with 1.2 g of iodate-free KI and the solids were dissolved with vigorous stirring into 10 mL of 1.0 M $HClO_4$. The resulting yellow-brown solution was diluted with 10 mL of deionized water and then titrated against a 0.01 M $Na_2S_2O_3$ solution that contained ca. 0.1 g of Na_2CO_3 and 3 drops of $CHCl_3$ per liter. Standardization of the sodium thiosulfate titrant was performed against a 2.000×10^{-3} M KIO_3 (Cerac, 99.9%) primary standard solution. Four drops of freshly prepared starch indicator (ca. 10 g L^{-1}) were added near the end of the titration, as was approximately 1 g of KSCN in order to discourage adsorption of triiodide ion by the CuI precipitate. At least three titrations were performed for each composition. The average values of the oxygen contents are reported in Tables 1 and 3; the errors in these values were obtained by propagating twice the standard deviation of the mean. (This error reflects only the statistical uncertainties of the titrations and excludes systematic errors arising from, for example, uncertainties in the assumed cation stoichiometry or the concentration of titrant.) We emphasize that no as-

(5) Soderholm, L.; Zhang, K.; Hinks, D. G.; Beno, M. A.; Jorgenson, J. D.; Segre, C. U.; Schuller, I. K. *Nature* **1987**, *328*, 604.
(6) Dalichaouch, Y.; Torikachvili, M. S.; Early, E. A.; Lee, B. W.; Seaman, C. L.; Yang, K. N.; Zhou, H.; Maple, M. B. *Solid State Commun.* **1988**, *65*, 1001.
(7) Lamberti, V. E.; Rodriguez, M. A.; Trybulski, J. D.; Navrotsky, A. *J. Mater. Res.* **1996**, *11*, 1061.
(8) Lamberti, V. E.; Rodriguez, M. A.; Navrotsky, A. *Powder Diffr.* **1995**, *10*, 297.
(9) Zhou, Z.; Navrotsky, A. *J. Mater. Res.* **1992**, *7*, 2920.
(10) Peters, D. G.; Hayes, J. M.; Hieftje, G. M. *Chemical Separations and Measurements: Theory and Practice of Analytical Chemistry*; Saunders: Philadelphia, 1974; pp 322−32.
(11) Nazzal, A. I.; Lee, V. Y.; Engler, E. M.; Jacowitz, R. D.; Tokura, Y.; Torrance, J. B. *Physica C* **1988**, *153−155*, 1367.
(12) Zakharchuk, N. F.; Fedina, T. P.; Borisova, N. S. *Superconductivity* **1991**, *4*, 1282.

Table 3. Oxygen Contents and Structural Characteristics of $Y_{1-x}Pr_xBa_2Cu_3O_{7-\delta}$ Compositions

x	$7-\delta$[a]	a (Å)	b (Å)	c (Å)	V (Å^3)	$100D$[b] (Å)	ΔV_m (Å^3)
0.0	6.974(6)	3.8193(5)	3.8876(6)	11.6807(14)	173.44(3)	6.83(8)	0
0.1	6.974(5)	3.8219(3)	3.8917(4)	11.6807(6)	173.74(2)	6.98(5)	−0.12(3)
0.2	6.972(5)	3.8249(2)	3.8945(2)	11.6856(4)	174.07(1)	6.96(3)	−0.21(3)
0.3	6.960(6)	3.8286(3)	3.8987(3)	11.6928(9)	174.53(2)	7.01(4)	−0.16(3)
0.4	6.953(5)	3.8326(5)	3.9024(6)	11.6957(13)	174.92(3)	6.98(8)	−0.19(4)
0.5	6.955(5)	3.8365(4)	3.9085(7)	11.6982(11)	175.41(3)	7.20(8)	−0.12(3)
0.6	6.945(4)	3.8416(5)	3.9121(5)	11.7015(10)	175.86(3)	7.05(7)	−0.09(3)
0.7	6.943(5)	3.8461(5)	3.9168(7)	11.7051(12)	176.33(3)	7.07(9)	−0.03(3)
0.8	6.968(6)	3.8492(4)	3.9210(5)	11.7103(9)	176.74(2)	7.18(6)	−0.04(2)
0.9	6.972(7)	3.8549(4)	3.9264(5)	11.7130(11)	177.29(2)	7.16(6)	0.08(2)
1.0	6.955(5)	3.8587(2)	3.9302(1)	11.7126(3)	177.62(1)	7.15(2)	0

[a] Error obtained through propagation of twice the standard deviation of the mean. [b] Orthorhombic distortion, $b - a$.

sumptions regarding the valence of Pr were made in applying this technique.

X-ray Diffraction. Structural information was obtained on a Scintag PAD V powder diffractometer controlled by a DEC MicroVAX 3100 computer. The diffractometer employed Cu Kα radiation and was fitted with a 25 cm horizontal goniometer and a Ge solid-state detector. (A more complete description of this instrument is available in ref 8.) Samples were mounted on zero-background (off-axis) quartz plates that had been thinly coated with Dow-Corning high-vacuum grease; the plates were rotated during data collection. Lattice parameters were typically refined from diffraction patterns that spanned 20−70° 2θ and were taken with a step size and count time of 0.02° 2θ and 3 s, respectively. All patterns were accumulated under ambient conditions. The observed d spacings were corrected with a second-order polynomial generated by calibration against NIST standard silicon (reference material 640b). The patterns were indexed with the aid of the resident program TREOR and then refined with a least-squares routine based on the LCLSQ (ver. 8.5) program of Burnham.[13] The refinements were performed within the orthorhombic *Pmmm* space group (No. 47) for the 123-class materials, and within the orthorhombic *Ammm* space group (No. 65) for the 124-class materials.

Calorimetry. Drop-solution oxide-melt calorimetry was performed on a Tian-Calvet-type calorimeter. This instrument and the various methodologies of oxide-melt calorimetry have been described in detail by Navrotsky.[14,15] Briefly, our experimental technique consisted of dropping a pressed, room-temperature sample pellet into a molten lead borate solvent ($Pb_2B_2O_5$) held at 976 K. The heat flow accompanying dissolution of the sample was measured by a Pt/Pt(13Rh) thermopile surrounding the reaction chamber and linking it to a constant-temperature Hastelloy block. At the end of the experiment, the integrated output of the thermopile was corrected for baseline instabilities and converted to energy—a quantity known as the *enthalpy of drop solution*, ΔH_{ds}—using a calibration factor independently determined with quarter-gram sections of high-purity platinum wire. Sample pellets measured 2.0 mm in diameter and were typically of mass 20 mg. A constant stream (∼30 mL/min) of dry air was maintained over the surface of the solvent in order to aid dissipation of evolved O_2 (vide infra). At least eight dissolutions were performed for each composition; no concentration or sample-size effects were observed.

Zhou et al.[9,16] have recently employed optical-absorption (Cu^{2+} at 13 800 cm^{-1}) and mass-change measurements to demonstrate that, under conditions identical with ours, the final dissolution products of both Y123 and Y124 in molten lead borate are ionic species corresponding to the compositions Y_2O_3, BaO, and CuO. The identities of the dissolution products of $YBa_2Cu_3O_{7-\delta}$ were independent of the value of δ.[9,16] To test our expectation that the title materials would behave in an analogous manner, we performed a series of experiments in which the changes in mass accompanying dissolution of selected Ln123 and Ln124 derivatives, including Pr123, were measured. The results of these experiments confirmed that the Ln123 and Ln124 dissolve completely as oxides of stoichiometry Ln_2O_3, BaO, and CuO well within the typical 60-minute data collection period. That is, the overall drop-solution reactions of the Ln123 and the Ln124 are

$$LnBa_2Cu_3O_{7-\delta}\,(s, 298\ K) \rightarrow {}^1/_2Ln_2O_3(d, 976\ K) + 2BaO(d, 976\ K) + 3CuO(d, 976\ K) + {}^1/_2(0.5-\delta)O_2(g, 976\ K)\uparrow \quad (1)$$

and

$$LnBa_2Cu_4O_8\,(s, 298\ K) \rightarrow {}^1/_2Ln_2O_3(d, 976\ K) + 2BaO(d, 976\ K) + 4CuO(d, 976\ K) + {}^1/_4O_2(g, 976\ K)\uparrow \quad (2)$$

respectively, where s represents a solid, g a gas, and d a dilute dissolved species. (Note that, for $6.5 < 7-\delta < 7.0$, dissolution of $PrBa_2Cu_3O_{7-\delta}$ into ionic species corresponding to Pr_2O_3, BaO, and CuO would result in a *negative* mass change, while dissolution into ionic species corresponding to PrO_2, BaO, and CuO would result in a *positive* mass change.) We emphasize again that no assumptions were made regarding the valence of Pr in Pr123 or, indeed, regarding the charge distributions within the 123 and 124 unit cells.

The enthalpy of drop solution can conveniently be thought to consist of two distinct contributions: (i) the heat required to bring the sample to the temperature of the calorimeter; (ii) the heat associated with the sample−solvent reaction at this temperature. For our materials, the latter reaction can itself be divided into two separate processes: (i) reduction of the sample with concomitant evolution of oxygen [$(0.5-\delta)/2$ mol O_2 for a 123-class compound and $^1/_4$ mol O_2 for a 124-class compound]; (ii) dissolution of the resulting composition. For purposes of comparison, the values of ΔH_{ds} for the high- and low-oxygen-content Ln123 compositions were normalized to $\delta = 0$ and $\delta = 0.5$, respectively, utilizing the appropriate enthalpies of oxidation. More positive enthalpies of dissolution generally correspond to more stable substances.

Thermochemical Calculations

Enthalpies of Formation. The molar enthalpies (or heats) of formation from the oxides at 298 K, ΔH_f^{ox}, were calculated from thermochemical cycles composed of the drop-solution reactions of the HTS and their component oxides. Each cycle was closed by a reaction (eq 8) representing the thermal equilibration of the oxygen voided by the HTS during dissolution. For example, the cycle employed for a Ln123 derivative ($\delta \leq 0.5$) was

(13) Burnham, C. W. *Carnegie Inst. Washington Yearbook* **1962**, *61*, 132.
(14) Navrotsky, A. *Phys. Chem. Miner.* **1977**, *2*, 89.
(15) Navrotsky, A., submitted to *Phys. Chem. Miner.*
(16) Zhou, Z.; McClure, D. S.; Navrotsky, A. *Phys. Chem. Glasses* **1993**, *34*, 251.

$$LnBa_2Cu_3O_{7-\delta}(s, 298\ K) \leftarrow {}^1/_2Ln_2O_3(d, 976\ K) + 2BaO(d, 976\ K) + 3CuO(d, 976\ K) + {}^1/_2(0.5 - \delta)O_2(g, 976\ K)\uparrow \quad (3)$$

$${}^1/_2Ln_2O_3(s, 298\ K) \rightarrow {}^1/_2Ln_2O_3(s, 976\ K) \quad (4)$$

$${}^1/_2Ln_2O_3(s, 976\ K) \rightarrow {}^1/_2Ln_2O_3(d, 976\ K) \quad (5)$$

$$2BaO(s, 298\ K) \rightarrow 2BaO(d, 976\ K) \quad (6)$$

$$3CuO(s, 298\ K) \rightarrow 3CuO(d, 976\ K) \quad (7)$$

$${}^1/_2(0.5 - \delta)O_2(g, 298\ K) \rightarrow {}^1/_2(0.5 - \delta)O_2(g, 976\ K) \quad (8)$$

$${}^1/_2Ln_2O_3(s, 298\ K) + 2BaO(s, 298\ K) + 3CuO(s, 298\ K) + {}^1/_2(0.5 - \delta)O_2(g, 298\ K) \xrightarrow{\Delta H_f^{ox}} LnBa_2Cu_3O_{7-\delta}(s, 298\ K)$$

For the 123-class materials, values are given in the tables only for $\delta = 0$, but can readily be calculated for any $\delta \leq 0.5$ through the cycle presented above and for any $\delta \geq 0.5$ through an analogous cycle that sums to[9]

$${}^1/_2Ln_2O_3(s, 298\ K) + 2BaO(s, 298\ K) + (\delta - 0.5)Cu_2O(s, 298\ K) + (4 - 2\delta)CuO(s, 298\ K) \xrightarrow{\Delta H_f^{ox}} LnBa_2Cu_3O_{7-\delta}(s, 298\ K)$$

The enthalpies of drop-solution for BaO, Cu_2O, and CuO (-91.5 ± 1.9, 129.0 ± 1.4, and 67.9 ± 0.6 kJ mol^{-1}, respectively) were taken from Zhou and Navrotsky.[9] A quantity equivalent to ΔH_{ds}, calculated by algebraically summing the heat content at 976 K (reaction 4) and the enthalpy of solution into $Pb_2B_2O_5$ at this temperature (reaction 5), was used for each of the Ln_2O_3 and for Y_2O_3. This procedure was adopted because pressed sesquioxide pellets dissolved intractably slowly in drop-solution experiments, probably due to local solvent saturation and consequent formation of metastable yttrium and rare-earth borates.[17] The heat contents of the sesquioxides, as well as that of molecular oxygen (21.86 ± 0.22 kJ mol^{-1} at 976 K), were obtained through integration of the constant-pressure heat capacity expressions tabulated by Robie et al.;[18] an uncertainty of $\pm 1\%$ was assumed in each case. The enthalpies of solution, ΔH_{sol}, were taken from Takayama-Muromachi and Navrotsky[19] with the exception of Pr_2O_3, which was excluded from the earlier study along with the La, Ce, Pm, and Tb congeners. The enthalpy of solution of Pr_2O_3 was estimated by means of a first-order regression of the $\Delta H_{sol}(Ln_2O_3)$ values provided by Takayama-Muromachi and Navrotsky[19] against the atomic number of the lanthanide. The enthalpies of formation from the elements at 298 K, ΔH_f^{el}, were obtained from the ΔH_f^{ox} by means of tabulated[18] elemental formation data of BaO, Cu_2O, CuO, and the sesquioxides.

(17) Bularzik, J.; Navrotsky, A.; DiCarlo, J.; Bringley, J.; Scott, B.; Traill, S. *J. Solid State Chem.* **1991**, *93*, 418.
(18) Robie, R. A.; Hemingway, B. S.; Fisher, J. R. *U. S. Geol. Survey Bull.* **1978**, *No. 1352*.
(19) Takayama-Muromachi, E.; Navrotsky, A. *J. Solid State Chem.* **1993**, *106*, 349.

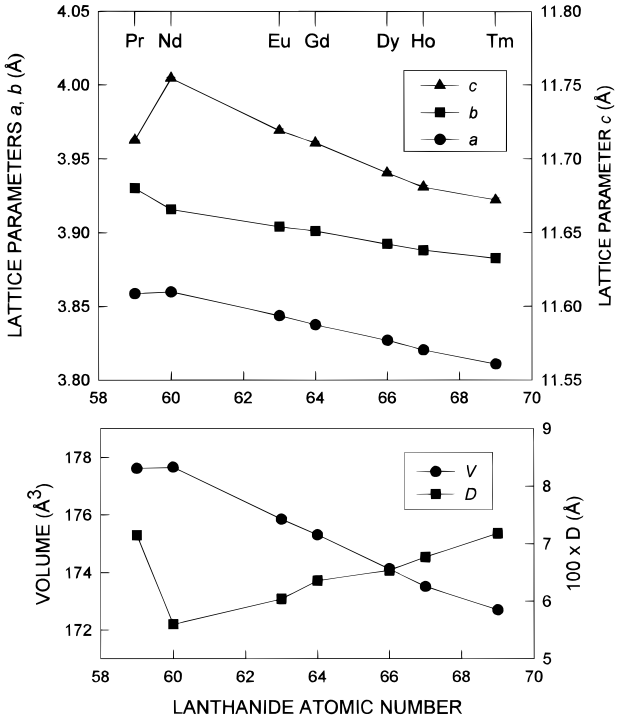

Figure 1. Lattice parameters, unit-cell volumes, and orthorhombic distortions of high-oxygen-content ($\delta < 0.7$) $LnBa_2Cu_3O_{7-\delta}$ derivatives plotted vs the atomic number of the lanthanide ion. The error bars are within the dimensions of the symbols.

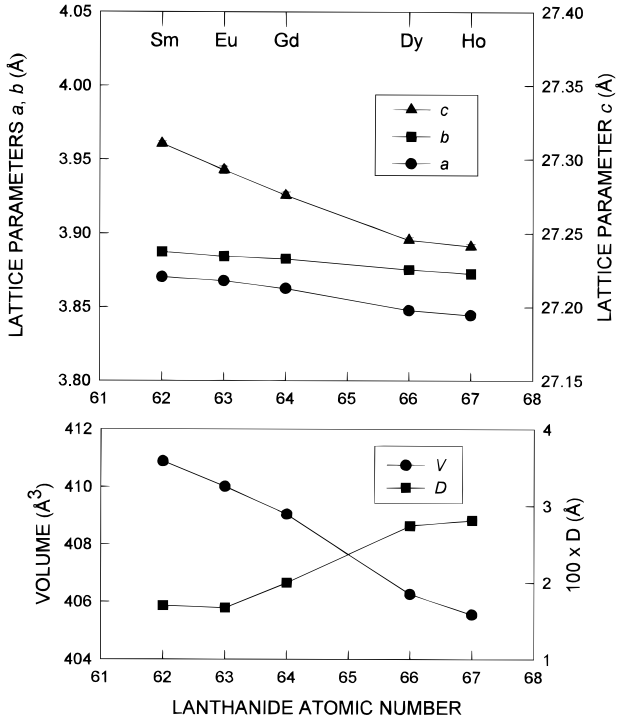

Figure 2. Lattice parameters, unit-cell volumes, and orthorhombic distortions of $LnBa_2Cu_4O_8$ derivatives plotted vs the atomic number of the lanthanide ion. The error bars are within the dimensions of the symbols.

Enthalpies of Oxidation. The partial molar enthalpy of oxidation at 298 K, $\Delta\bar{h}_O$, of each 123-class compound was determined by first calculating the enthalpy required to increase the oxygen content of the compound from $7 - \delta$ to $7 - \eta$ atoms per unit cell (ΔH_{ox}) and then dividing by the difference in oxygen content

(enthalpies of oxidation are conventionally expressed per mol O):

$$LnBa_2Cu_3O_{7-\delta}(s, 298\ K) \rightarrow {}^1/_2Ln_2O_3\ (d, 976\ K) + 2BaO(d, 976\ K) + 3CuO(d, 976\ K) + {}^1/_2(0.5 - \delta)O_2(g, 976\ K)\uparrow \quad (9)$$

$$LnBa_2Cu_3O_{7-\eta}(s, 298\ K) \leftarrow {}^1/_2Ln_2O_3(d, 976\ K) + 2BaO(d, 976\ K) + 3CuO(d, 976\ K) + {}^1/_2(0.5 - \eta)O_2(g, 976\ K)\uparrow \quad (10)$$

$${}^1/_2(\eta - \delta)O_2(g, 298\ K) \rightarrow {}^1/_2(\eta - \delta)O_2(g, 976\ K) \quad (11)$$

$$LnBa_2Cu_3O_{7-\delta}(s, 298\ K) + {}^1/_2(\eta - \delta)O_2(g, 298\ K) \xrightarrow{\Delta H_{ox}} LnBa_2Cu_3O_{7-\eta}(s, 298\ K)$$

$$\Delta\bar{h}_O = \Delta H_{ox}/(\eta - \delta) \quad (12)$$

Enthalpies of the 123−124 Reactions. The change in enthalpy accompanying the solid-state reaction of CuO with $LnBa_2Cu_3O_7$ to form $LnBa_2Cu_4O_8$ at 298 K was calculated utilizing the drop-solution data for CuO and both classes of HTS:

$$LnBa_2Cu_3O_7(s, 298\ K) \rightarrow {}^1/_2Ln_2O_3(d, 976\ K) + 2BaO(d, 976\ K) + 3CuO(d, 976\ K) + {}^1/_4O_2(g, 976\ K)\uparrow \quad (13)$$

$$LnBa_2Cu_4O_8(s, 298\ K) \leftarrow {}^1/_2Ln_2O_3(d, 976\ K) + 2BaO(d, 976\ K) + 4CuO(d, 976\ K) + {}^1/_4O_2(g, 976\ K)\uparrow \quad (14)$$

$$CuO(s, 298\ K) \rightarrow CuO(d, 976\ K) \quad (15)$$

$$LnBa_2Cu_3O_7(s, 298\ K) + CuO(s, 298\ K) \xrightarrow{\Delta H_{123-124}} LnBa_2Cu_4O_8(s, 298\ K)$$

Enthalpies of Mixing. The molar enthalpies of mixing at 298 K of the fully oxygenated $Y_{1-x}Pr_xBa_2Cu_3O_{7-\delta}$ solid solutions were determined by algebraically summing the enthalpies of drop-solution of the (Y,Pr)123 compositions and hypothetical mechanical mixtures composed of x mol of Pr123 and $(1 - x)$ mol of Y123:

$$Y_{1-x}Pr_xBa_2Cu_3O_7(s, 298\ K) \leftarrow (x/2)Pr_2O_3(d, 976\ K) + ((1 - x)/2)Y_2O_3(d, 976\ K) + 2BaO(d, 976\ K) + 3CuO(d, 976\ K) + {}^1/_4O_2(g, 976\ K)\uparrow \quad (16)$$

$$xPrBa_2Cu_3O_7(s, 298\ K) + (1 - x)YBa_2Cu_3O_7(s, 298\ K) \rightarrow (x/2)Pr_2O_3(d, 976\ K) + ((1 - x)/2)Y_2O_3(d, 976\ K) + 2BaO(d, 976\ K) + 3CuO(d, 976\ K) + {}^1/_4O_2(g, 976\ K)\uparrow \quad (17)$$

$$xPrBa_2Cu_3O_7(s, 298\ K) + (1 - x)YBa_2Cu_3O_7(s, 298\ K) \xrightarrow{\Delta H_{mix}} Y_{1-x}Pr_xBa_2Cu_3O_7(s, 298\ K)$$

Consistent with the absence of concentration or sample-size effects, we have assumed dilute-solution conditions in this calculation, which effectively means that the enthalpy of drop-solution of a mechanical mixture of end-members is identical with the weighted average of the end-member enthalpies.

Results and Discussion

Structural Considerations. The 123 and 124 phases comprise two ($n = 0$ and 2, respectively) of the three superconducting phases identified to date in the $R_2Ba_4Cu_{6+n}O_{14+n-\delta}$ system. [The third superconducting phase, $R_2Ba_4Cu_7O_{15-\delta}$ ($n = 1$), occurs as an ordered intergrowth between 123-like and 124-like structural slabs.] The structure of the 124 phase is similar to that of the 123 phase except that a second Cu(1)−O(1) layer, translated by $b/2$ along the **b** axis, is present in the 124 structure, more than doubling its unit-cell volume and increasing its symmetry from *Pmmm* to *Ammm*.[20−22] [The apical, or bridging, oxygen is designated O(4) in our notation.] Each O(1) atom in a 124-class compound is coordinated by three copper atoms rather than two, leading to an essentially stable oxygen content up to the decomposition temperature[22−24] and, consequently, to the absence of a thermally activated orthorhombic−tetragonal transition.[22,25] Phase equilibrium studies have indicated that Y124 is stable below ca. 1123 K at an oxygen pressure of 1 atm,[26−28] but conventional solid-state synthesis at this pressure occurs very slowly without added rate enhancers such as alkali carbonates.[29] Preparation of Ln124 derivatives with lanthanide ions larger than Eu^{3+} has been effected only under high oxygen pressure.[30,31]

Structural characteristics of the high-oxygen-content Ln123 derivatives, Ln124 derivatives, and high-oxygen-content (Y,Pr)123 solid solutions are presented in Figures 1−3 and Tables 1−3, respectively. Lattice parameters, unit-cell volumes, and orthorhombic distortions ($D \equiv b - a$) are given for each composition, and volumes of mixing (ΔV_m) are provided for the (Y,Pr)-123 solid solutions. In discussing these quantities, we must keep in mind that, even though each compound retains the general symmetry of its yttrium-based parent, most structural measures of a 123-class HTS are strongly dependent upon the oxygen content of its unit cell. Hence, we limit ourselves to a few broad

(20) Park, C.; Snyder, R. L. *J. Am. Ceram. Soc.* **1995**, *78*, 3171.
(21) Kaldis, E.; Fischer, P.; Hewat, A. W.; Hewat, E. A.; Karpinski, J.; Rusiecki, S. *Physica C* **1989**, *159*, 668.
(22) Berastegui, P.; Johansson, L.-G.; Käll, M.; Börjesson, L. *Physica C* **1992**, *204*, 147.
(23) Adachi, S.; Adachi, H.; Setsune, K.; Wasa, K. *Physica C* **1991**, *175*, 523.
(24) Karpinski, J.; Kaldis, E.; Jilek, E.; Rusiecki, S.; Bucher, B. *Nature* **1988**, *336*, 662.
(25) Meen, T.-H.; Chen, Y.-C.; Liaw, K.-W.; Yang, H.-D. *J. Am. Ceram. Soc.* **1993**, *76*, 1948.
(26) Pooke, D.; Buckley, R. G.; Presland, M. R.; Tallon, J. L. *Phys. Rev. B* **1990**, *41*, 6616.
(27) Morris, D. E.; Markelz, A. G.; Fayn, B.; Nickel, J. H. *Physica C* **1990**, *168*, 153.
(28) Wada, T.; Suzuki, N.; Ichinose, A.; Yaegashi, Y.; Yamauchi, H.; Tanaka, S. *Appl. Phys. Lett.* **1990**, *57*, 81.
(29) Cava, R. J.; Krajewski, J. J.; Peck, W. F., Jr.; Batlogg, B.; Rupp, L. W., Jr.; Fleming, R. M.; James, A. C. W. P.; Marsh, P. *Nature* **1989**, *338*, 328.
(30) Rao, C. N. R.; Nagarajan, R.; Vijayaraghavan, R. *Superconduct. Sci. Technol.* **1993**, *6*, 1.
(31) Morris, D. E.; Nickel, J. H.; Wei, J. Y. T.; Asmar, N. G.; Scott, J. S.; Scheven, U. M.; Hultgren, C. T.; Markelz, A. G.; Post, J. E.; Heaney, P. J.; Veblen, D. R.; Hazen, R. M. *Phys. Rev. B* **1989**, *39*, 7347.

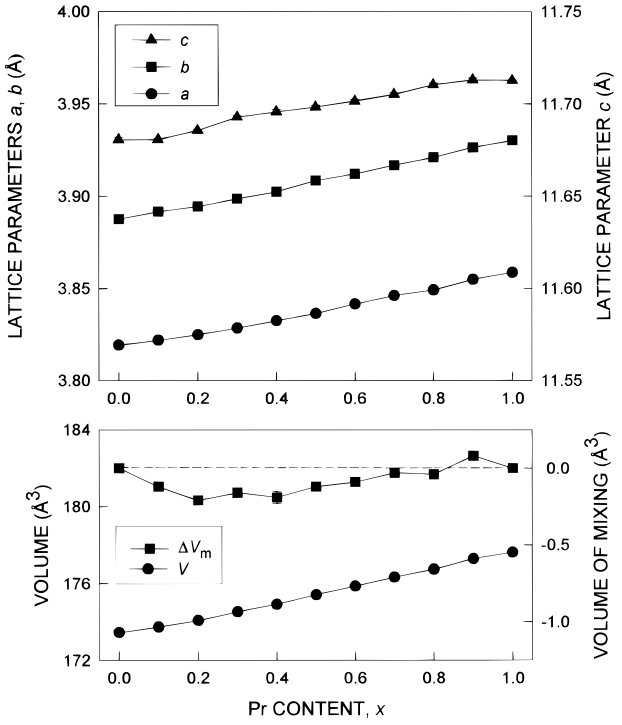

Figure 3. Lattice parameters, unit-cell volumes, and volumes of mixing of high-oxygen-content ($\delta < 0.7$) $Y_{1-x}Pr_xBa_2Cu_3O_{7-\delta}$ solid solutions plotted vs x. With one exception, the error bars are within the dimensions of the symbols.

observations that do not rely upon rigorous comparisons of the values of δ—and do not involve the introduction of questionable approximations.

(i) With a few exceptions—a number of early studies,[32,33] for example, classified the symmetry of Pr123 as tetragonal—the lattice parameters and unit-cell volumes of our materials agree with those reported previously for the Ln123 derivatives,[32−40] Ln124 derivatives,[23,31,41−44] and (Y,Pr)123 solid solutions.[4,45−48]

(ii) If the figures corresponding to the Ln123 and Ln124 derivatives are drawn to the same scale, the plots of lattice parameter a vs lanthanide atomic number are nearly superimposable across the series from Eu to Ho, as are the plots of b vs lanthanide atomic number. The c lattice parameter and the unit-cell volume decrease more rapidly for the Ln124 but display greater percentage changes for the Ln123.

(iii) As also reported earlier, the orthorhombic distortions of the Ln123[32,33,35] and Ln124[23,31,41,43,44] derivatives increase with decreasing atomic number of the lanthanide ion. The values of D for the Ln123 are larger by more than a factor of 2 than those for the Ln124 but appear to increase less rapidly toward the right of the lanthanide period.

(iv) The overall structural trends of the Ln123 derivatives are all broken to a lesser or greater extent at the Pr-containing congener. While it might be tempting to interpret these anomalies in terms of a mixed Pr^{3+}/Pr^{4+} state, this course of action should be approached with caution, since, as pointed out by Guillaume[35] et al., valence states in the 123 structure should properly be inferred from interionic distances due to the complexity of the unit cell.

(v) The volumes of mixing of the $Y_{1-x}Pr_xBa_2Cu_3O_{7-\delta}$ solid solutions

$$\Delta V_m(x) \equiv V(x) - (1 - x)V_{Y123} - xV_{Pr123} \qquad (18)$$

exhibit asymmetric negative deviations from ideality, with the greater departures occurring for the yttrium-rich compositions. These deviations do not correspond to the small differences in oxygen content between the samples, as can be demonstrated through a plot of δ vs x (not shown).

Thermochemistry of $LnBa_2Cu_3O_{7-\delta}$ Derivatives. The enthalpies of drop-solution of the high- and low-oxygen-content Ln123 derivatives are presented in Table 4 and Figure 4. [As mentioned above, the values of ΔH_{ds} for the high- and low-oxygen-content compositions were normalized to $\delta = 0$ and $\delta = 0.5$, respectively. The same treatment was given to the (Y,Pr)123 drop-solution data presented below.] The two sets of ΔH_{ds} are quite similar in form and display a slight endothermic trend with decreasing lanthanide radius (increasing lanthanide atomic number). Other properties of the 123-class superconductors, perhaps most notably the critical transition temperature, are similarly relatively insensitive to the choice of lanthanide.[32,40] Both curves exhibit a double-peaked structure about the analogue based on the spherically symmetric ($4f^7$) Gd^{3+} ion; the doublet structure is somewhat exaggerated for the low-oxygen-content samples. Takayama-Muromachi and Navrotsky[19] have rationalized similar trends in the heats of solution of Ln_2O_3 in molten $Pb_2B_2O_5$ in terms of cubic crystal-field stabilization energies. Unlike the situation for the structural parameters (vide supra), the values of ΔH_{ds} for the Pr congener follow the trends established by the other Ln123. Consistency between Pr123 and the other lanthanide derivatives of Y123 has also been noted for the separations between the copper−oxygen planes (the so-called slot widths)[36,37] and for the unit-cell volumes,[47] both of which increase with lanthanide radius.

(32) Tarascon, J. M.; McKinnon, W. R.; Greene, L. H.; Hull, G. W.; Vogel, E. M. *Phys. Rev. B* **1987**, *36*, 226.
(33) LePage, Y.; Siegrist, T.; Sunshine, S. A.; Schneemeyer, L. F.; Murphy, D. W.; Zahurak, S. M.; Waszczak, J. V.; McKinnon, W. R.; Tarascon, J. M.; Hull, G. W.; Greene, L. H. *Phys. Rev. B* **1987**, *36*, 3617.
(34) Malik, S. K.; Yelon, W. B.; Rhyne, J. J.; James, W. J.; Prasad, R.; Adhikary, K.; Soni, N. C. *Solid State Commun.* **1994**, *89*, 383.
(35) Guillaume, M.; Allenspach, P.; Mesot, J.; Roessli, B.; Staub, U.; Fisher, P.; Furrer, A. *Z. Phys. B* **1993**, *90*, 13.
(36) Lowe-Ma, C. K.; Vanderah, T. A. *Physica C* **1992**, *201*, 233.
(37) López-Morales, M. E.; Ríos-Jara, D.; Tagüeña, J.; Escudero, R.; La Placa, S.; Bezinge, A.; Lee, V. Y.; Engler, E. M.; Grant, P. M. *Phys. Rev. B* **1990**, *41*, 6655.
(38) Li, W.-H.; Lynn, J. W.; Skanthakumar, S.; Clinton, T. W.; Kebede, A.; Jee, C.-S.; Crow, J. E.; Mihalisin, T. *Phys. Rev. B* **1989**, *40*, 5300.
(39) Ganguli, A. K.; Rao, C. N. R.; Sequeira, A.; Rajagopal, H. *Z. Phys. B* **1989**, *74*, 215.
(40) Lin, J. G.; Huang, C. Y.; Xue, Y. Y.; Chu, C. W.; Cao, X. W.; Ho, J. C. *Phys. Rev. B* **1995**, *51*, 12900.
(41) Mori, K.; Kawaguchi, Y.; Ishigaki, T.; Katano, S.; Funahashi, S.; Hamaguchi, Y. *Physica C* **1994**, *219*, 176.
(42) Kakihana, M.; Yoshimura, M.; Mazaki, H.; Yasuoka, H.; Nishio, S.; Suzuki, Y.; Börjesson, L.; Käll, M. *J. Alloys Compd.* **1993**, *193*, 132.
(43) Miyatake, T.; Kosuge, M.; Wada, T.; Yaegashi, Y.; Yamauchi, H.; Koshizuka, N.; Murayama, C.; Mori, N. In *Proceedings of the 5th International Symposium on Superconductivity*; Bando, Y., Yamauchi, H., Eds.; Springer: Tokyo, 1993.
(44) Fisher, P.; Roessli, B.; Mesot, J.; Allenspach, P.; Staub, U.; Kaldis, E.; Bucher, B.; Karpinski, J.; Rusiecki, S.; Jilek, E.; Hewat, A. W. *Physica B* **1992**, *180, 181*, 414.
(45) Booth, C. H.; Bridges, F.; Boyce, J. B.; Claeson, T.; Zhao, Z. X.; Cervantes, P. *Phys. Rev. B* **1994**, *49*, 3443.
(46) Neumeier, J. J.; Bjørnholm, T.; Maple, M. B.; Rhyne, J. J.; Gotaas, J. A. *Physica C* **1990**, *166*, 191.

Table 4. Thermodynamic Functions of $LnBa_2Cu_3O_{7-\delta}$ Compositions

Ln	$\Delta H_{ds}^{\delta=0}$ (kJ/mol)[a]	$\Delta H_{ds}^{\delta=0.5}$ (kJ/mol)[a]	ΔH_f^{ox} (kJ/mol)[b,c]	ΔH_f^{el} (kJ/mol)[b,c]	$\Delta \bar{h}_O$ (kJ/mol O)[b]
Pr	164.52 ± 1.03	112.75 ± 2.37	−137.9 ± 11.4	−2610.8 ± 13.1	−94.9 ± 6.4
Nd	167.64 ± 2.56	122.47 ± 2.61	−141.7 ± 5.7	−2613.9 ± 8.0	−82.7 ± 10.1
Eu	172.94 ± 2.04	129.05 ± 2.12	−134.4 ± 4.7	−2528.2 ± 8.4	−77.8 ± 6.5
Gd	162.11 ± 1.99	114.19 ± 1.56	−131.4 ± 5.0	−2609.4 ± 7.7	−85.7 ± 5.5
Dy	167.85 ± 2.46	117.91 ± 2.18	−123.6 ± 4.9	−2623.3 ± 7.7	−91.8 ± 8.7
Ho	172.26 ± 2.96	136.00 ± 3.48	−129.1 ± 5.9	−2637.6 ± 8.4	−63.0 ± 10.4
Tm	168.89 ± 2.37	121.05 ± 2.56	−123.3 ± 5.0	−2635.8 ± 7.5	−86.9 ± 8.6

[a] Error represents twice the standard deviation of the mean. [b] Error obtained through propagation of twice the standard deviation of the mean. [c] Enthalpies of formation refer to an oxygen content of 7 atoms/formula unit.

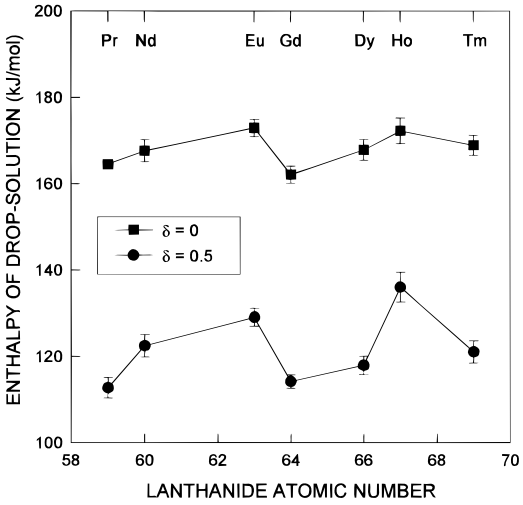

Figure 4. Enthalpies of drop-solution of $LnBa_2Cu_3O_{7-\delta}$ derivatives plotted vs the atomic number of the lanthanide ion. The solvent was a $Pb_2B_2O_5$ melt held at 976 K. The error bars represent twice the standard deviation of the mean.

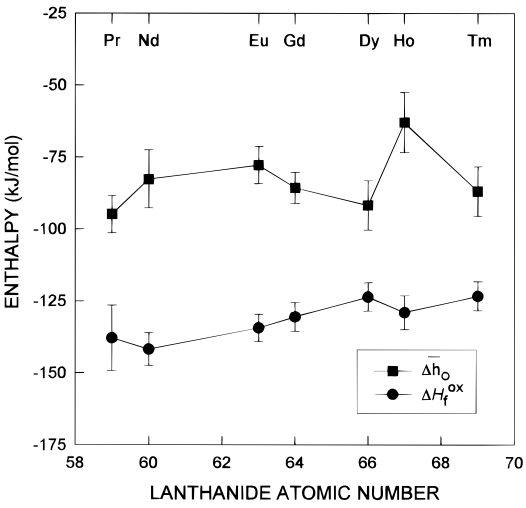

Figure 5. Enthalpies of formation from the oxides at 298 K ($\delta = 0$) and partial molar enthalpies of oxidation at 298 K of $LnBa_2Cu_3O_{7-\delta}$ derivatives plotted vs the atomic number of the lanthanide ion. The error bars were obtained through propagation of twice the standard deviation of the mean.

The enthalpies of formation from the oxides at 298 K (ΔH_f^{ox}) and the partial molar enthalpies of oxidation at 298 K ($\Delta \bar{h}_O$) of the Ln123 are presented in Table 4 and Figure 5. (As mentioned in the section detailing the thermochemical calculations, the enthalpies of formation refer to an oxygen content of 7 atoms/formula unit. In general, the enthalpy of formation of a 123-class HTS becomes more exothermic with increasing oxygen content.) The enthalpies of formation display an essentially linear trend toward less exothermic values with increasing lanthanide atomic number, implying that the Ln123 become more stable with increasing lanthanide radius. The structural data indicate that the orthorhombic distortion increases, but the unit-cell volume decreases, with increasing lanthanide atomic number. The heats of oxidation, in contrast, are essentially independent of the choice of lanthanide, suggesting that the chain-site charge distributions of the Ln123 are comparable. As noted for the high- and low-oxygen-content values of ΔH_{ds}(Pr123), the values of ΔH_f^{ox}(Pr123) and $\Delta \bar{h}_O$(Pr123) are consistent with the trends defined by the other Ln123.

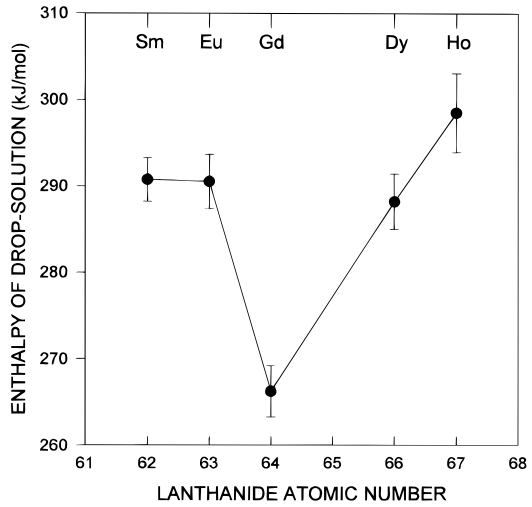

Figure 6. Enthalpies of drop-solution of $LnBa_2Cu_4O_8$ derivatives plotted vs the atomic number of the lanthanide ion. The solvent was a $Pb_2B_2O_5$ melt held at 976 K. The error bars represent twice the standard deviation of the mean.

Thermochemistry of $LnBa_2Cu_4O_8$ Derivatives. The enthalpies of drop-solution and formation from the oxides at 298 K of the 124-class lanthanide derivatives are displayed in Figures 6 and 7, respectively, and Table 5. A number of comparisons with the Ln123 data can be drawn even though the present series is more limited in breadth. The enthalpies of drop-solution of the Ln124 evince the same general trends as their 123-class counterparts, with the minimum again occurring at the Gd congener. These similarities almost certainly derive from the identical local environments of the lanthanide sites in the two cuprate structures. We recall that the trends in the orthorhombic distortions and unit-cell volumes of the Ln124 derivatives are also very similar to those of the Ln123 derivatives. The (average) values of the ΔH_{ds}(Ln124) are approximately 1.6−1.7 times the values of the corresponding ΔH_{ds}(Ln123), a result reminiscent of the nearly constant ratio of the unit-cell

(47) Kebede, A.; Jee, C. S.; Schwegler, J.; Crow, J. E.; Mihalisin, T.; Myer, G. H.; Salomon, R. E.; Schlottmann, P.; Kuric, M. V.; Bloom, S. H.; Guertin, R. P. *Phys. Rev. B* **1989**, *40*, 4453.

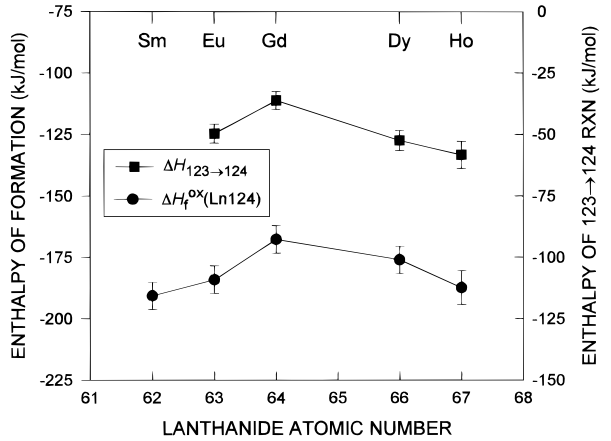

Figure 7. (i) Enthalpies of formation from the oxides at 298 K of $LnBa_2Cu_4O_8$ derivatives; and (ii) enthalpies accompanying the reactions Ln123(s) + CuO(s) → Ln124(s) at 298 K, both plotted vs the atomic number of the lanthanide ion. The error bars were obtained through propagation of twice the standard deviation of the mean.

Table 5. Thermodynamic Functions of $LnBa_2Cu_4O_8$ Compositions

Ln	ΔH_{ds} (kJ/mol)[a]	ΔH_f^{ox} (kJ/mol)[b]	ΔH_f^{el} (kJ/mol)[b]	$\Delta H_{123-124}$ (kJ/mol)[b]
Sm	290.77 ± 2.54	−190.6 ± 5.6	−2827.6 ± 8.5	
Eu	290.53 ± 3.17	−184.1 ± 5.6	−2735.3 ± 9.4	−49.7 ± 3.8
Gd	266.25 ± 2.95	−167.7 ± 5.6	−2803.0 ± 8.7	−36.2 ± 3.6
Dy	288.20 ± 3.21	−176.1 ± 5.6	−2833.1 ± 8.7	−52.4 ± 4.1
Ho	298.50 ± 4.58	−187.4 ± 7.0	−2853.2 ± 9.8	−58.3 ± 5.5

[a] Error represents twice the standard deviation of the mean. [b] Error obtained through propagation of twice the standard deviation of the mean.

volumes of the two classes of HTS ($V_{Ln124}/V_{Ln123} \approx 2.3$). In contrast, the enthalpies of formation of the Ln124 derivatives bear little resemblance to the ΔH_f^{ox}(Ln123), and, rather than a roughly linear dependence upon the atomic number (or effective ionic radius) of the lanthanide, manifest a maximum at Gd124. The values of the enthalpic ratio $\Delta H_f^{ox}(Ln124)/\Delta H_f^{ox}$(Ln123) are still effectively constant, however, and all fall in the range 1.3−1.4.

The Ln123−Ln124 Reaction. Also shown in Figure 7 and Table 5 are the enthalpies accompanying the reactions Ln123(s) + CuO(s) → Ln124(s) at 298 K, $\Delta H_{123-124}$. These quantities exhibit the same overall trends as the enthalpies of formation of the Ln124 derivatives, including a maximum at Ln = Gd. The qualitative similarities between the $\Delta H_{123-124}$ and the ΔH_f^{ox}(Ln124) are not completely surprising—in addition to the method outlined above, but with significantly larger uncertainties, the changes in enthalpy accompanying the Ln123−Ln124 reactions could have been calculated by subtracting the enthalpies of formation of the fully oxygenated Ln123, which vary only slightly over the sequence Eu−Ho, from the corresponding enthalpies of formation of the Ln124. (This can be readily verified by constructing a thermochemical cycle from the formation reactions of the two classes of HTS.) The values of $\Delta H_{123-124}$ are of the same (exothermic) sign and magnitude as the enthalpy accompanying the Y123−Y124 reaction (−31.9 ± 22.3 kJ mol^{-1}),[9] implying that, like Y124, each Ln124 derivative is stable with respect to an assemblage of its fully oxygenated 123 phase and CuO.

The $Y_{1-x}Pr_xBa_2Cu_3O_{7-\delta}$ System. $PrBa_2Cu_3O_{7-\delta}$ ($\delta \approx 0$) exhibits a variety of physical and structural anomalies that distinguish it from the other rare-earth derivatives of Y123. In addition to the absence of any superconducting phase,[5,6] these anomalies include a heavy-fermion-like specific heat [$\gamma_0 \approx 200$ mJ K^{-2} (mol Pr)$^{-1}$],[49] enhanced magnetic transition widths in inelastic neutron scattering spectra,[50] a rare-earth polyhedral volume significantly smaller than that of Nd123,[36] and subtle contractions in the Cu(2)−O(4)[36,45,51] and Pr−O(2)[35] bond lengths. One especially interesting feature is an antiferromagnetic ordering[38] of the Pr sublattice at 17 K—a value more than an order of magnitude greater than that obtained from a de Gennes extrapolation[47] of the lanthanide ordering temperatures of the other Ln123—that is accompanied by a change in entropy of approximately $R \ln 2$.[47,52] $PrBa_2Cu_4O_8$ (Pr124) has also been reported to display an absence of superconductivity to temperatures as low as 2 K.[53−55]

In the hope that an understanding of the unusual characteristics of Pr123 will lead to new ideas about the mechanism of high-T_c superconductivity, as well as to improved practical devices such as nearly-lattice-matched S−I−S junctions, many theoretical and experimental investigations have been performed upon this material and its analogues. (See, for example, the review by Radousky.[4]) Most discussions of the structure and physics of Pr123 have been framed in terms of the formal valence of the Pr ion (3+, intermediate, or 4+).[4,36,37,50,56,57] Models based on a formal Pr valence at or near 3.0 generally rely upon hybridization between the Pr 4f states and the conduction band. In contrast, arguments that favor tetravalent Pr generally assume that the additional dissociated electron of this ion is affiliated with the copper−oxygen planes, where superconductivity is destroyed by electron−hole recombination. The hybridization picture appears to be supported by the majority of experiments and calculations,[4,58] and, indeed, superconductivity suppression, abnormal magnetic properties, and heavy-fermion behavior are well-known in compounds in which the Pr ion is without question trivalent.[59] However, it must also be admitted that the superconducting critical temperatures of the Ln123 derivatives increase slightly with lanthanide radius[32,40] and that the effective ionic radii of Pr are only about 1% larger than those of Nd for all common

(48) Felner, I.; Yaron, U.; Nowick, I.; Bauminger, E. R.; Wolfus, Y.; Yacoby, E. R.; Hilscher, G.; Pillmayr, N. *Phys. Rev. B* **1989**, *40*, 6739.
(49) Phillips, N. E.; Fisher, R. A.; Caspary, R.; Amato, A.; Radousky, H. B.; Peng, J. L.; Zhang, L.; Shelton, R. N. *Phys. Rev. B* **1991**, *43*, 11 488.
(50) Hilscher, G.; Holland-Moritz, E.; Holubar, T.; Jostarndt, H.-D.; Nekvasil, V.; Schaudy, G.; Walter, U.; Fillion, G. *Phys. Rev. B* **1994**, *49*, 535.
(51) Kinoshita, K.; Matsuda, A.; Shibata, H.; Ishii, T.; Watanabe, T.; Yamada, T. *Jpn. J. Appl. Phys.* **1988**, *27*, L1642.
(52) Jee, C. S.; Kebede, A.; Nichols, D.; Crow, J. E.; Mihalisin, T.; Myer, G. H.; Perez, I.; Salomon, R. E.; Schlottmann, P. *Solid State Commun.* **1989**, *69*, 379.
(53) Nobuaki, S.; Terasaki, I.; Adachi, S.; Yamauchi, H. *ISTEC J.* **1995**, *8*, 24.
(54) Yamada, Y.; Horii, S.; Yamada, N.; Guo, Z.; Kodama, Y.; Kawamoto, K.; Mizutani, U.; Hirabayashi, I. *Physica C* **1994**, *231*, 131.
(55) Nobuaki, S.; Adachi, S.; Yamauchi, H. *Physica C* **1994**, *227*, 377.
(56) Soderholm, L.; Loong, C.-K.; Goodman, G. L.; Dabrowski, B. D. *Phys. Rev. B* **1991**, *43*, 7923.
(57) Khomskii, D. *J. Superconduct.* **1993**, *6*, 69.
(58) Guo, G. Y.; Temmerman, W. M. *Phys. Rev. B.* **1990**, *41*, 6372.
(59) Sampathkumaran, E. V. *Physica B* **1992**, *176*, 217.
(60) Shannon, R. D. *Acta Crystallogr.* **1976**, *A32*, 751.

Table 6. Thermodynamic Functions of $Y_{1-x}Pr_xBa_2Cu_3O_{7-\delta}$ Compositions

x	$\Delta H_{ds}^{\delta=0}$ (kJ/mol)[a]	$\Delta H_{ds}^{\delta=0.5}$ (kJ/mol)[a]	ΔH_f^{ox} (kJ/mol)[b,c]	ΔH_f^{el} (kJ/mol)[b,c]	$\Delta \bar{h}_O$ (kJ/mol O)[b]
0.0	172.73 ± 2.41	114.54 ± 2.19	−136.7 ± 4.9	−2657.5 ± 7.5	−106.8 ± 7.5
0.1	168.31 ± 1.75	112.67 ± 1.62	−133.2 ± 4.7	−2649.2 ± 7.3	−103.1 ± 6.2
0.2	163.68 ± 2.90	111.90 ± 1.41	−129.5 ± 5.6	−2640.7 ± 7.9	−94.3 ± 7.6
0.5	154.88 ± 2.47	109.68 ± 1.98	−123.5 ± 7.2	−2620.4 ± 9.2	−80.6 ± 7.1
0.8	155.44 ± 1.15	117.06 ± 1.58	−126.9 ± 9.5	−2609.4 ± 11.3	−70.4 ± 5.8
0.9	158.53 ± 1.92	116.41 ± 1.15	−130.9 ± 10.5	−2608.7 ± 12.3	−75.9 ± 5.8
1.0	164.52 ± 1.03	112.75 ± 2.37	−137.9 ± 11.4	−2610.8 ± 13.1	−94.9 ± 6.4

[a] Error represents twice the standard deviation of the mean. [b] Error obtained through propagation of twice the standard deviation of the mean. [c] Enthalpies of formation refer to an oxygen content of 7 atoms/formula unit.

coordination numbers,[60] meaning that a considerably more subtle microscopic description may be needed. In perhaps the most sophisticated approach to date, Fehrenbacher and Rice[61] have theoretically modeled the electronic structure of Pr123 in terms of mixed-valent Pr configurations, insulating CuO_2 planes, and CuO_3 chains described by a one-dimensional $t-J$ model. The lanthanide ion is almost certainly trivalent in the Nd, Gd, Ho, Er, and Yb derivatives.[62]

Experimental investigations of Pr123 have often centered on the $R_{1-x}Pr_xBa_2Cu_3O_{7-\delta}$ solid solutions, in which R is Y or, less commonly, another stable lanthanide. The value of T_c decreases monotonically with x in each of these series, becoming undetectable at a critical value (x_c) that varies with R. For R = Y, $x_c \approx 0.55$.[5,6] $T_c(x)$ data reported by Xu and Guan,[63] Malik[64] et al., and others suggest that the depressions of the critical temperatures of these systems are at least partially consistent with the Abrikosov−Gor'kov[65] (AG) pair-breaking theory, which treats the destruction of superconductivity in terms of exchange scattering of conduction electrons by localized magnetic moments. The AG theory must be applied with some caution, however, as there is little understanding[66] even of the appearance of *semi*conductivity in the (Y, Pr)123 system near $x = 0.5$.[6,47,52,67] (Intriguingly, Pr124 is *metallic* at temperatures less than 170 K.[53]) An analogous depression of T_c with Pr content has been reported for $Y_{1-x}Pr_xBa_2Cu_4O_8$, with x_c in the neighborhood of 0.8.[22,25,68,69]

Our thermodynamic data for the (Y, Pr)123 solid solutions are presented in Table 6 and Figures 8−11. The two series of drop-solution data ($\delta = 0$, 0.5), shown in Figure 8, display several striking differences. The values of ΔH_{ds} corresponding to the high-oxygen-content samples exhibit asymmetric negative deviations from the ideal line joining the two end-members, suggesting that substitution of Pr into Y123 and substitution of Y into Pr123 are both significantly destabilizing. Comparing the high- and low-x extremes of this plot, the greater initial destabilization results from the introduction of the Y^{3+} ion, whose effective radius in 8-fold coordination (1.019 Å) is smaller than that of Pr^{3+} (1.126 Å) but greater than that of Pr^{4+} (0.96 Å).[60] The continuous nature of the data argues against any sudden valence instability at this level of oxygenation, a conclusion also drawn by Kebede et al.[47] on the basis of smooth expansions of the lattice parameters with increasing x. The values of ΔH_{ds} corresponding to the low-oxygen-content samples show negative deviations from ideality for x less than about 0.6 and positive deviations thereafter, implying that substitution of Pr into Y123 is initially destabilizing and substitution of Y into Pr123 is initially stabilizing in this regime. The departures from ideality of the low-oxygen-content samples are substantially smaller in magnitude than

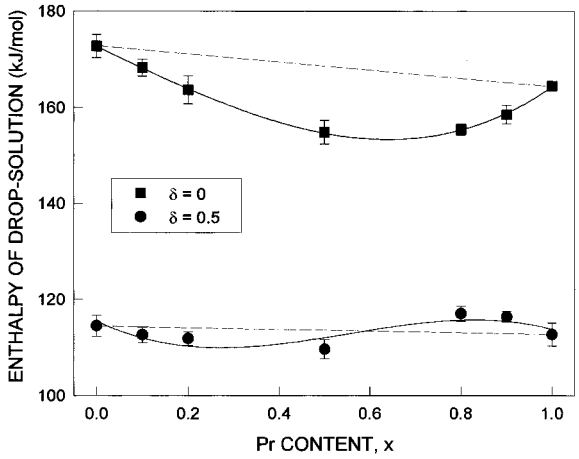

Figure 8. Enthalpies of drop-solution of $Y_{1-x}Pr_xBa_2Cu_3O_{7-\delta}$ solid solutions plotted vs x. The solvent was a $Pb_2B_2O_5$ melt held at 976 K. The dashed lines represent ideal solid solutions, while the solid lines were calculated from third-order regression functions. The error bars extend to twice the standard deviation of the mean.

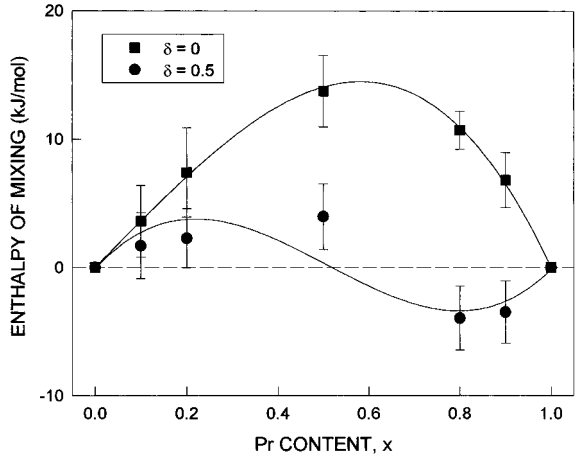

Figure 9. Enthalpies of mixing at 298 K of $Y_{1-x}Pr_xBa_2Cu_3O_7$ solid solutions plotted vs x. The solid lines were calculated from third-order regression functions constrained to pass through zero at the end-members. The error bars were obtained through propagation of twice the standard deviation of the mean.

(61) Fehrenbacher, R.; Rice, T. M. *Phys. Rev. Lett.* **1993**, *70*, 3471.
(62) Nagoshi, M.; Fukuda, Y.; Suzuki, T. *J. Electron. Spectrosc. Relat. Phenom.* **1994**, *66*, 257.
(63) Xu, Y.; Guan, W. *Physica C* **1991**, *183*, 105.
(64) Malik, S. K.; Tomy, C. V.; Bhargava, P. *Phys. Rev. B* **1991**, *44*, 7042.
(65) Abrikosov A. A.; Gor'kov, L. P. *Zh. Eksp. Teor. Fiz.* **1961**, *39*, 1781 [*Sov. Phys. JETP* **1961**, *12*, 1243].
(66) Abrikosov, A. A., private communication.
(67) Peng, J. L.; Klavins, P.; Shelton, R. N.; Radousky, H. B.; Hahn, P. A.; Bernardez, L. *Phys. Rev. B* **1989**, *40*, 4517.

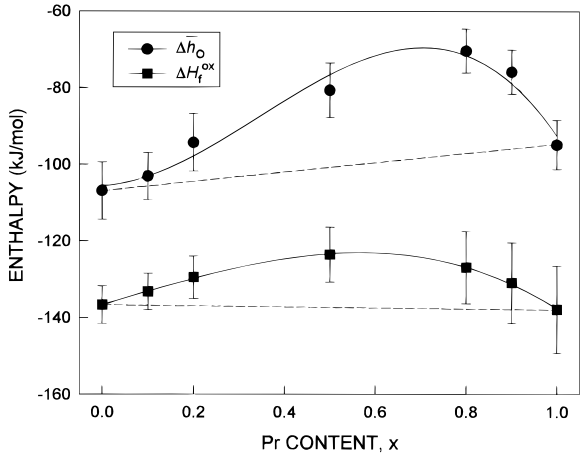

Figure 10. Enthalpies of formation from the oxides at 298 K ($\delta = 0$) and partial molar enthalpies of oxidation at 298 K of $Y_{1-x}Pr_xBa_2Cu_3O_{7-\delta}$ solid solutions plotted vs x. The dashed lines represent ideal solid solutions, while the solid lines were calculated from third-order regression functions. The error bars were obtained through propagation of twice the standard deviation of the mean.

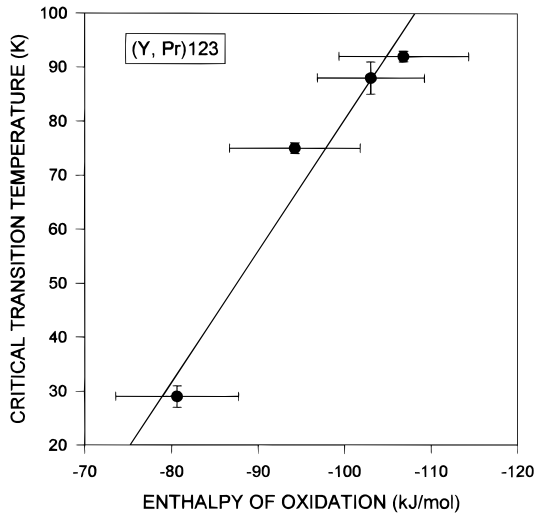

Figure 11. Dependence of the superconducting critical temperatures of high-oxygen-content $Y_{1-x}Pr_xBa_2Cu_3O_{7-\delta}$ solid solutions upon $\Delta\bar{h}_O(x)$. The solid line represents a first-order regression function with slope -2.4 K mol kJ^{-1}. The error bars extend to twice the standard deviation of the mean in both directions; to provide a more reliable estimate of the errors in the critical temperatures, the values of $T_c(x)$ represent averages of data of five studies.[5,47,85−87]

those of the high-oxygen-content samples. The differences between the two series of data are almost certainly related to the expansion in unit-cell volume that accompanies deoxygenation of the 123 structure,[37] which leads to a roomier and perhaps more flexible lattice for the samples with oxygen contents near 6.5 atoms/unit cell. The distinctive T_c vs x relationship[5,6] is not reflected in either series of enthalpies.

The enthalpies of mixing at 298 K of the high- and low-oxygen-content solid solutions, ΔH_m, are displayed in Figure 9. As expected from the drop-solution data, the values of ΔH_m are consistently endothermic (positive) for the high-oxygen-content compounds but show both endothermic and exothermic domains for the low-oxygen-content materials. (The volumes of mixing, it should be remembered, are consistently negative across the series for $\delta = 0$.) Adopting the common practice for mixing data exhibiting substantial asymmetry, we have modeled the system within the subregular approximation:[70−73]

$$\Delta H_m = X_Y X_{Pr}(X_Y W^H_{Pr} + X_{Pr} W^H_Y) \qquad (19)$$

where X_i is the mole fraction of species i and W^H_i, the *enthalpic interaction parameter*, depends only upon temperature and pressure. The form of this equation is ultimately based upon Margules' series representation of the partial vapor pressure of a binary liquid solution[74] and can be interpreted as a linear combination of the excess enthalpic components of two regular solutions.[72] Following Waldbaum and Thompson,[70] we fitted the enthalpies of mixing for each oxygen content to a third-order polynomial:

$$\Delta H_m(X_{Pr}) = A + BX_{Pr} + CX_{Pr}^2 + DX_{Pr}^3 \qquad (20)$$

which, because ΔH_m vanishes by definition at both end-members, we constrained to pass through zero at $X_{Pr} = 0.0$ and 1.0 by imposing the conditions $A = A + B + C + D = 0$. Then, as may be verified by expanding eq 19 in terms of X_{Pr}, we obtained the interaction parameters as

$$W^H_Y = -(C + 2D) \qquad (21a)$$

$$W^H_{Pr} = -(C + D) \qquad (21b)$$

Mixing curves calculated from the regression functions are displayed as solid lines in Figure 9. The interaction parameters are $W^H_Y = 76 \pm 20$ and $W^H_{Pr} = 36 \pm 32$ kJ mol^{-1} for $\delta = 0$, and $W^H_Y = -35 \pm 25$ and $W^H_{Pr} = 39 \pm 24$ kJ mol^{-1} for $\delta = 0.5$. The uncertainties in these quantities were obtained in the manner of Pawley[75] et al. Although mixing studies involving the exchange of trivalent ions are rather scarce in the literature, the values for the high-oxygen-content series are similar to those reported by Chatterjee et al. for mixing of Al_2O_3 and Cr_2O_3 corundums[76] and $MgAl_2O_4$ and $MgCr_2O_4$ spinels.[77]

The enthalpies of formation from the oxides at 298 K ($\delta = 0$) and the partial molar enthalpies of oxidation at 298 K of the (Y,Pr)123 solid solutions are displayed in Figure 10. Both sequences of data exhibit asymmetric endothermic deviations from ideality, with the greater deviations again occurring for the yttrium-rich phases. (The large errors in the values of ΔH_f^{ox} result from our least-squares estimation of the heat of solution of Pr_2O_3.) The shapes of the curves imply that introduction of Y

(68) Adachi, S.; Watanabe, N.; Seiji, N.; Koshizuka, N.; Yamauchi, H. *Physica C* **1993**, 207, 127.
(69) Herrmann, J.; Boehnke, U.-C.; Krötzsch, M.; Lippold, B.; Schlenkrich, F. *Physica C* **1994**, *221*, 76.
(70) Waldbaum, D. R.; Thompson, J. B., Jr. *Am. Mineral.* **1968**, *53*, 2000.
(71) Thompson, J. B., Jr. In *Researches in Geochemistry II*; Abelson, P. H., Ed.; John Wiley & Sons: New York, 1967; pp 340−361.
(72) Grover, J. In *Thermodynamics in Geology*; Fraser, D. G., Ed.; D. Reidel: Dordrecht-Holland, 1977; pp 67−97.
(73) Hardy, H. K. *Acta Met.* **1953**, *1*, 202.
(74) Margules, M. *S. B. Wien Akad.* **1895**, *104*, 1243.
(75) Pawley, A. R.; Graham, C. M.; Navrotsky, A. *Am. Mineral.* **1993**, *78*, 23.
(76) Chatterjee, N. D.; Leistner, H.; Terhart, L.; Abraham, K.; Klaska, R. *Am. Mineral.* **1982**, *67*, 725.
(77) Oka, Y.; Steinke, P.; Chatterjee, N. D. *Contrib. Mineral. Petrol.* **1984**, *87*, 196.

into the Pr123 structure lessens the stabilizing effect of oxygenation, as well as the stability of the 123 phase itself, more than introduction of Pr into the Y123 structure. The enhanced destabilization at high x may reflect disruption of additional bonding interactions that derive from the f-electron density of Pr. In addition, this effect—or at least its magnitude—may be unique to the Pr-containing systems: comparative crystal-chemical data of the Ln123, particularly the lengths of the Cu(2)−O(4)[36,45,51] and Ln−O(2)[35] bonds, indicate that the oxygen network is anomalously contracted about the Pr site in Pr123. Lütgemeier[78] has presented NMR/NQR data suggesting that the charge distribution at the Cu(1) site of the $Y_{1-x}Pr_xBa_2Cu_3O_{7-\delta}$ system is not a sensitive function of x.

After correction for oxygen content, the enthalpy of formation of Y123 agrees within the limits of its error with previously reported values.[9,79−82] [References 80−82 require the correction discussed by Voronin and Degterov (Degtyarev)[83,84] for the enthalpy change accompanying the reaction $Cu(ClO_4)_2{\cdot}6H_2O(s) = Cu(ClO_4)_2(aq) + 6H_2O(aq)$.] The partial molar enthalpy of oxidation of Y123 is also consistent with previously reported values.[9,79,80] Comparison of the thermodynamic properties of Y123 with those of Ho123, however, leads to an intriguing discrepancy: the effective radii of the trivalent yttrium and holmium ions in 8-fold coordination are nearly identical, as are the unit-cell volumes and orthorhombic distortions of Y123 and Ho123, but the partial molar enthalpy of oxidation of Ho123 is significantly more endothermic than that of Y123. We interpret this difference as another indication of the importance of covalent bonding in the high-T_c cuprates, with the interactions this time mediated by the f-electron density of the holmium ion.

We have also observed that the superconducting critical temperatures of the high-oxygen-content $Y_{1-x}Pr_xBa_2Cu_3O_{7-\delta}$ solid solutions depend in a linear fashion upon $\Delta\bar{h}_O(x)$. This relationship, illustrated in Figure 11, provides a connection between the superconducting properties and the chain-site energetics of the (Y,Pr)123 system, at least for the yttrium-rich phases: the critical temperature is highest for the composition that is most stabilized by oxygenation at the O(4) site or, equivalently, by the introduction of holes. [To provide a more reliable estimate of the errors in the critical temperatures, the values of $T_c(x)$ in Figure 11 represent averages of data of five studies.[5,47,85−87]]

Collectively, our results imply thermodynamic similarity of $PrBa_2Cu_3O_{7-\delta}$ and the other members of the 123 class of quaternary oxides, as well as the absence of any gross energetic anomaly associated with the suppression of superconductivity in Pr123. Our thermodynamic data also lend support for the predominance of trivalent Pr across the $Y_{1-x}Pr_xBa_2Cu_3O_{7-\delta}$ series, and suggest that the critical temperatures of the (Y,Pr)123 solid solutions are linearly dependent upon $\Delta\bar{h}_O(x)$. Unfortunately, little can be said at this point about the universality of the link between T_c and $\Delta\bar{h}_O$. The body of thermochemical knowledge of the high-temperature superconductors must be expanded before the significance of the relationship between T_c and $\Delta\bar{h}_O$ can be fully appreciated, especially with respect to the substitution of Pr for other species with f-electron density.

Acknowledgment. The authors are grateful to Dr. G. A. Rossetti, Jr., for critical insights into the structural analysis, to Dr. L. Topor for tireless counsel on the calorimetry, and to Dr. E. A. Smelik for help in searching the mineralogical literature. This work was supported by DOE Grant DE-FGO2-89ER45394 and by the New Jersey BISEC Teacher Improvement Project.

CM9604928

(78) Lütgemeier, H. *J. Magn. Magn. Mater.* **1990**, *90, 91*, 633.
(79) Parks, M. E.; Navrotsky, A.; Mocala, K.; Takayama-Muromachi, E.; Jacobson, A.; Davies, P. K. *J. Solid State Chem.* **1989**, *79*, 53; *erratum* **1989**, *83*, 218.
(80) Morss, L. R.; Sonnenberger, D. C.; Thorn, R. J. *Inorg. Chem.* **1988**, *27*, 2106.
(81) Brosha, E. L.; Davies, P. K.; Garzon, F. H.; Raistrick, I. D. *Science* **1993**, *260*, 196.
(82) Garzon, F. H.; Raistrick, I. D.; Ginley, D. S.; Halloran, J. W. *J. Mater. Res.* **1991**, *6*, 885.
(83) Voronin, G. F.; Degterov, S. A. *Physica C* **1991**, *176*, 387.
(84) Degtyarev, S. A.; Voronin, G. F. *Russ. J. Phys. Chem.* **1993**, *67*, 1217.
(85) Maple, M. B.; Paulius, L. M.; Neumeier, J. J. *Physica C* **1992**, *195*, 64.
(86) Liu, H. B., unpublished data.
(87) Nieva, G.; Ghamaty, S.; Lee, B. W.; Maple, M. B.; Schuller, I. L. *Phys. Rev. B* **1991**, *44*, 6999.